



Synthesis and characterization of H-ZSM-5/[AI]MCM-41 microporous-mesoporous hybrid materials

Jorge Arce-Castro^{1,2}, Gabrielle S. de Aquino², Ana Beatriz M. Bastos², Raildo A. Fiuza-Junior^{1,2,3}, Delano M. de Santana^{1,4}, Mauricio B. dos Santos^{1,2}, Fernanda T. Cruz^{1,2}, Silvio A. B. V. de Melo^{1,5}, Artur J. S. Mascarenhas^{1,2,3,*}

- ¹ Programa de Pós-Graduação em Energia e Ambiente (PGENAM), Escola Politécnica, Universidade Federal da Bahia, R. Prof. Aristides Novis, 2, Federação, 40120-910, Salvador BA, Brasil.
- ² Laboratório de Catálise e Materiais (LABCAT), Departamento de Química Geral e Inorgânica, Instituto de Química, Universidade Federal da Bahia, Travessa Barão de Jeremoabo, 147, Campus Ondina, 40170-280, Salvador BA, Brasil.
- ³ Programa de Pós-Graduação em Química (PGQUIM), Instituto de Química, Universidade Federal da Bahia, Rua Barão de Jeremoabo, 147 Campus Universitário de Ondina CEP: 40.170-115, Salvador BA, Brasil.
- ⁴Laboratório de Energia e Gás (LEN), Escola Politécnica, Universidade Federal da Bahia, R. Prof Aristides Novis, 2 Federação, 40120-910, Salvador-BA, Brasil.
- ⁵ Laboratório de Nanotecnologia Supercrítica (LNS), Centro Interdisciplinar de Energia e Ambiente (CIENAM), R. Barão de Jeremoabo, S/N, Campus de Ondina, 40170-115, Salvador-BA, Brasil.

*e-mail: artur@ufba.br

Resumo/Abstract

RESUMO - Neste trabalho, o híbrido H-ZSM-5/[A1]MCM-41 foi preparado a partir do zeólito H-ZSM-5 pré-sintetizado, usando CTABr como direcionador de estrutura. A difração de raios X confirmou a manutenção da fase MFI (ZSM-5), enquanto se forma a mesofase hexagonal ([A1]MCM-41), resultando na combinação de ambas no híbrido. A análise térmica possibilitou identificar a adequada temperatura de calcinação para completa remoção do CTA⁺. As razões molares SiO₂/Al₂O₃ determinadas por FRX foram 24,6, 32,2 e 23,8, respectivamente, para o H-ZSM-5, o MCM-41 e o híbrido. As micrografias eletrônicas revelaram que o H-ZSM-5 é formado por cristais poliédricos hexagonais, enquanto o [A1]MCM-41 apresenta uma estrutura de tubos, e o híbrido parece ser uma mistura entrelaçada das duas morfologias. A fisissorção de N₂ mostrou áreas BET de 343, 854 e 483 m²g⁻¹, respectivamente, e a análise de porosidade indicou 16,3% de microporos e 83,7% de mesoporos no híbrido. Esses materiais são promissores como catalisadores ou suportes.

Palavras-chave: peneiras moleculares, híbrido microporoso-mesoporoso, síntese, caracterização.

ABSTRACT – In this work, H-ZSM-5/[Al]MCM-41 hybrid material was prepared by using a as-synthesized H-ZSM-5 zeolite, using CTABr as structure directing agent. X-ray diffraction confirmed the preservation of the MFI phase (ZSM-5), while the formation of the hexagonal mesophase (MCM-41) was also observed, resulting in the combination of both structures in the hybrid material. Thermal analysis enabled the identification of the appropriate calcination temperature for the complete removal of CTA⁺. The SiO₂/Al₂O₃ molar ratios determined by XRF were 24.6, 32.2, and 23.8, respectively, for H-ZSM-5, MCM-41 and the hybrid. The SEM micrographs revealed hexagonal polyhedral crystals for H-ZSM-5, a tubular morphology for [Al]MCM-41 and the hybrid appears to be an interwoven mixture of the two morphologies. Nitrogen physisorption showed BET surface areas of 343, 854, and 483 m²g⁻¹, and the hybrid exhibited 16.3% micropores and 83.7% mesopores. These materials are promising as catalysts or catalyst supports.

Keywords: molecular sieves, microporous-mesoporous hybrid, synthesis, characterization.

Introduction

Microporous and mesoporous materials, as well as hierarchical porous materials have attracted a great attention in the scientific community, because of their applicability in catalyst and adsorption technologies. It is possible to combine different properties of high surface area and acidity from the microporous zeolite together with the wide pore

system of the MCM-41 mesoporous material, giving interesting potential for catalytic applications (1).

Mesoporous zeolites have gained considerable attention from researchers in materials science and catalysis, both in academia and industry. Although pure siliceous [Al]MCM-41 mesoporous materials possess a neutral framework with weak surface acidity, this property limits their potential for commercial applications in areas such as catalysis, selective



adsorption, catalyst support, and adsorption processes. Even with the incorporation of heteroatoms, Al-containing mesoporous MCM-41 exhibits lower acidity and reduced thermal and hydrothermal stability compared to microporous zeolites (2,3). Nonetheless, few recent studies have explored the properties and synergistic effects resulting from the combination of crystalline phases characterized by high surface acidity and micropores smaller than 1.0 nm, with non-crystalline components exhibiting moderate surface acidity and mesopores within the 2.0 to 50 nm range, according to IUPAC classification (4-6).

In this work, a preparation route of a microporous/mesoporous hybrid material was prepared combining ZSM-5 zeolite and MCM-41 mesoporous material.

Experimental

The methodology was divided into stages: first, the synthesis of the microporous material; second, the mesoporous material; and finally, the hybrid material (microporous and mesoporous) was obtained, with all materials subsequently characterized by different techniques.

Materials

The reagents used were as follow: NaOH (Sigma Aldrich), cetyltrimethylammonium bromide-CTABr ($\hat{E}xodo\ científica \geq 98\%$), TEOS (Sigma-Aldrich $\geq 98\%$), ammonium nitrate (Synth, for analysis), Silica Aerosil 200 (Synth), H-Y (LABCAT-UFBA), sodium aluminate (Riedel-de Haen), acetic acid (Sigma-Aldrich, 98%), and distilled water.

Synthesis of ZSM-5 zeolite by interzeolite conversion

To convert Y zeolite into ZSM-5 zeolite, the method described by dos Santos et al. (7) was followed with some modifications. A total of 3.8 g of the starting material, in the acidic form (H-Y), was used along with 2.04 g of NaOH in 92 mL of H₂O under stirring. Then, an additional 2.04 g of NaOH was added to maintain a NaOH/SiO2 ratio of 0.3, followed by the addition of 9.8572 g of Aerosil 200 silica (Sigma-Aldrich). The mixture was stirred (300 rpm) for 30 min at room temperature. The resulting gel was transferred to a stainless steel autoclave and subjected to hydrothermal treatment for 5 days at 150°C. After the synthesis time, the autoclave was cooled, and the solid was filtered, washed with deionized water until pH = 7, and dried at 100° C. Ion exchange was performed to replace sodium with ammonium cationa using 0.1 mol L-1 NH4NO3 (Synth), adding 100 mL of solution per gram of zeolite. The suspension was stirred for 24 h at room temperature, then filtered and dried at



100°C. Finally, the sample was calcined with a heating rate of 1°C min⁻¹ up to 500°C under a nitrogen flow of 50 mL min⁻¹. After reaching 500°C, the gas was switched to synthetic air, and the temperature was maintained for 3 h.

Synthesis of the mesoporous material [Al]MCM-41

The synthesis of the mesoporous material was develop fallowing the methodology described by Pastore et al. (8).

Synthesis of hybrid material ZSM-5/[Al]MCM-41

For the synthesis of the hybrid material, the method from (8), was used as a basis for the formation of the mesoporous material, with the addition of previously synthesized H-ZSM-5 (SiO₂/Al₂O₃ = 24.6). Part of the aluminum came from the synthesized zeolite, and then adjusted with NaAlO₂, and the silica content was adjusted with the addition of TEOS, to achieve a final material ratio of SiO₂/Al₂O₃ = 30. The stoichiometric composition of the synthesis gel was:

NaOH: 0.0334 Al₂O₃: SiO₂: 0.5 CTABr: 100 H₂O

The material was synthesized by adding 1.67 g of NaOH and 0.20 g of NaAlO₂ to 80 mL of H₂O. After dissolution, 8.09 g of the surfactant prepared the day before, at a 50% solution. After homogenization, H-ZSM-5 was added and TEOS was added dropwise. The pH was then adjusted to approximately 10.80 with 98% glacial acetic acid, and stirring was maintained for additional 4 h. The gel was then transferred to an autoclave and submitted static hydrothermal treatment for 48 h at 100°C. Finally, the autoclave was cooled, the pH of the medium was measured, and vacuum filtration was performed, where the solid was washed until it stopped foaming and dried at 100°C for 6 h, and the solution was reserved for reuse.

Characterization

All materials were characterized by XRD using a Shimadzu XRD6000 equipment, which operates with $CuK\alpha$ radiation generated at 40 kV, 30 mA, and a graphite monochromator, in the 20 range of 1.4 to 50°. Fourier Transformed Infrared spectra (FTIR) was collected in a Perkin Spectrum 400 Elmer spectrometer. Thermogravimetric curves were obtained using a Shimadzu TGA-60H equipment, with a temperature range of 25 to 1000°C and a heating rate of 10°C min⁻¹, under a nitrogen flow of 50 mL min⁻¹. Elemental analyses were performed by X-ray Fluorescence (XRF-WD) on a Bruker WD-FRX S8-Tiger equipment, using a voltage of 40 kV and a current of 30 mA. Morphological analyses of the materials were carried out using a scanning electron microscope (SEM), model Hitachi S-3400N. The nitrogen adsorption isotherms were collected using the Micromeritics ASAP 2020 equipment, at a temperature of -196°C.



Results and discussion

X-ray diffraction (XRD)

Figure 1A shows the XRD patterns of the fully crystalline Na-ZSM-5 zeolite, freshly synthesized via interzeolite transformation using acidic H-Y zeolite as a precursor, without a structure-directing agent, resulting in a sustainable, environmentally friendly synthesis. After synthesis, ion exchange and calcination at 500°C were performed to obtain the acidic form. The MFI-type structure was confirmed by comparison with the IZA standard.

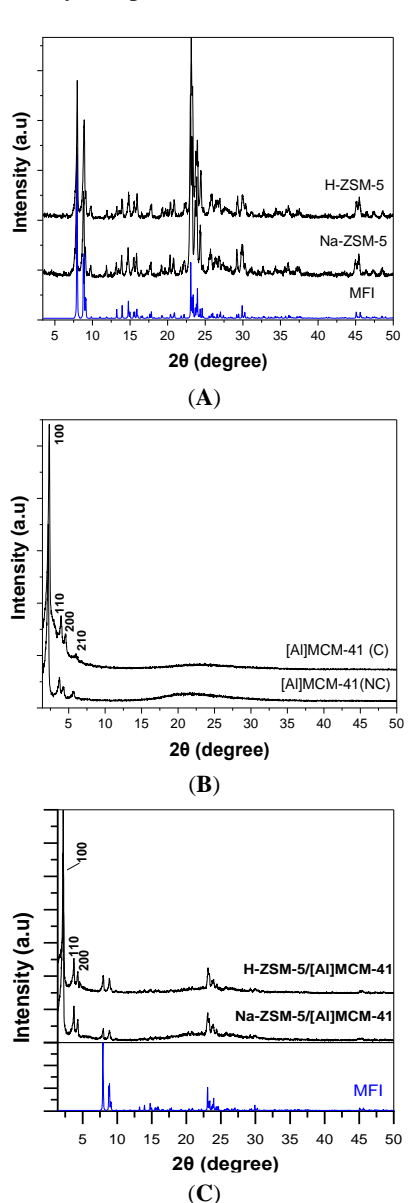


Figure 1. Powder X-ray diffraction patterns of samples: **A**: ZSM-5; **B**: [Al]MCM-41; **C**: ZSM-5/[Al]MCM-41.

In Figure 1B, pure phases are observed in the freshly synthesized samples, non-calcined (NC), along with an



amorphous halo between $2\theta = 15-30^{\circ}$. After calcination (C), the removal of the organic template is confirmed. The four characteristic reflection peaks of [Al]MCM-41—(100), (110), (200), and (210)—are present in both the assynthesized and calcined samples, consistent with previous studies (8,9).

Figure 1.C confirms the formation of the hybrid H-ZSM-5/MCM-41 material. At low angles, three characteristic [Al]MCM-41 reflections are observed, while at higher angles, the MFI-type structure from H-ZSM-5 is detected. After calcination and ion exchange, the expected phases were maintained, confirming structural stability of the material despite minor changes following thermal treatments.

Thermogravimmetry

The thermogravimmetric curves of the materials under an inert atmosphere are shown in Figure 2.

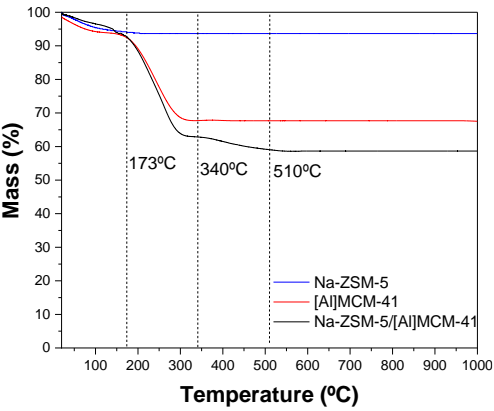


Figure 2. Thermogravimmetric curves of the materials. Conditions: mass = 5 mg; heating rate $b = 10^{\circ}$ C min⁻¹; N_2 flow = 50 mL min⁻¹.

The Na-ZSM-5 zeolite (blue curve) exhibits a single event between 50–200 °C, corresponding to the desorption of physisorbed water from the pores, with a mass loss of 6.34%. The mesoporous material [Al]MCM-41 (red curve) displays two distinct thermal events: (i) 63–150°C, associated with the loss of physisorbed water and volatile compounds, with a mass loss of approximately 7%; (ii) At 253°C, shows a mass loss of 30.13%, attributed to the decomposition of the surfactant CTABr used during synthesis.

The black curve, corresponding to the hybrid micro/mesoporous material Na-ZSM-5/[Al]MCM-41, reveals three main mass loss events with increasing temperature. The first, between 30–120°C, corresponds to a 6.2% mass loss due to the elimination of physisorbed water and other volatile species occluded in the micropores and mesopores. The second, between 120–339°C, results in a 29.12% mass loss, attributed to the thermal decomposition



of the organic structure-directing agent used to develop mesopores. The third event, occurring between 332–510°C, shows a 1.5% mass loss, associated with the dehydroxylation of surface sylanol (Si–OH) groups.

Figure 3 presents the FTIR spectra of the materials.

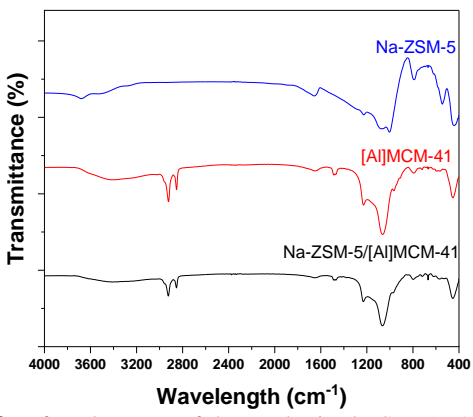


Figure 3. Infrared spectra of the synthesized ZSM-5, [Al]MCM-41 and H-ZSM-5/[Al]MCM-41 hybrid material.

The broad band between 3300–3700 cm⁻¹ corresponds to Si–OH and Si–OH–Al groups, as well as OH groups bonded to multivalent cations compensating the negative framework charge. For the [Al]MCM-41 and Na-ZSM-5/[Al]MCM-41 samples, bands at 2926, 2850, 1477, and 720 cm⁻¹ were observed, corresponding to the vibrational deformation of C–H bonds in CH₂ and CH₃ groups, confirming the presence of the organic structure-directing agent CTABr, as reported by reference (10).

Additionally, in all spectra, weak, medium, and strong bands are observed between 1200–400 cm⁻¹, characteristic of the asymmetric and symmetric stretching vibrations of Si(Al)O₄ tetrahedra due to external and internal vibrations, typical of these materials.

Electron microscopy

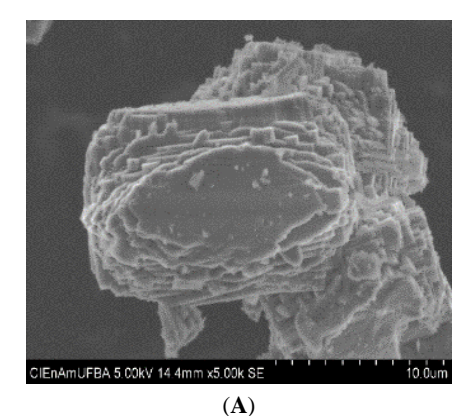
Figure 4 shows the micrographs of the materials at different magnifications.

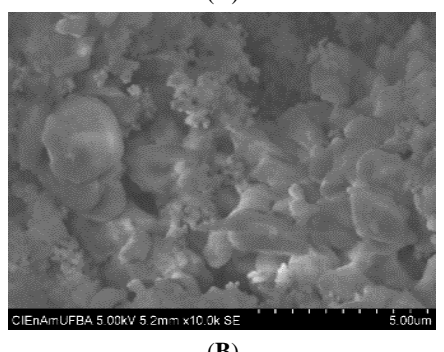
For Na-ZSM-5 (Figure 4.A), plate-like aggregates forming hexagonal polyhedra, characteristic of ZSM-5 zeolite morphology, can be observed, in agreement with previous studies (7).

For [Al]MCM-41 (Figure 4.B), the presence of rod- or tube-shaped clusters, as well as irregular agglomerates, can be seen. Similar results were reported in the literature (11).

In Figure 3.C, the presence of ZSM-5 characteristic polyhedra and interwoven rods is observed, suggesting the formation of the Na-ZSM-5/[Al]MCM-41 composite material.







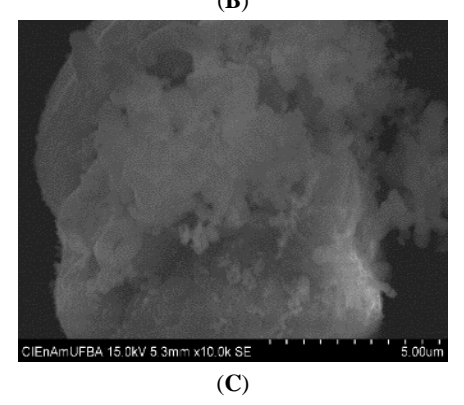


Figure 4. Scanning electron micrographs of the synthesized materials **A**: H-ZSM-5; **B**: [Al]MCM-41; C:_H-ZSM-5/[Al]MCM-41.

Elemental analysis by XRF

After calcination, the SiO₂/Al₂O₃ molar ratios were determined by X-ray fluorescence, as shown in Table 1. **Table 1.** Composition of samples by WD-XRF.

Samples	SiO ₂ /Al ₂ O ₃ (nominal)	SiO ₂ /Al ₂ O ₃ (experimental)
Na-ZSM-5	30	24.70
H-ZSM-5	30	24.58
[Al]MCM-41	30	32.20
Na-ZSM-5/[Al]MCM-41	30	23.80

All samples were synthesized with a nominal SiO_2/Al_2O_3 molar ratio of 30, the experimental values obtained by chemical analysis showed slight deviations. For Na-ZSM-5, H-ZSM-5, and the hybrid Na-ZSM-5/[Al]MCM-41, the



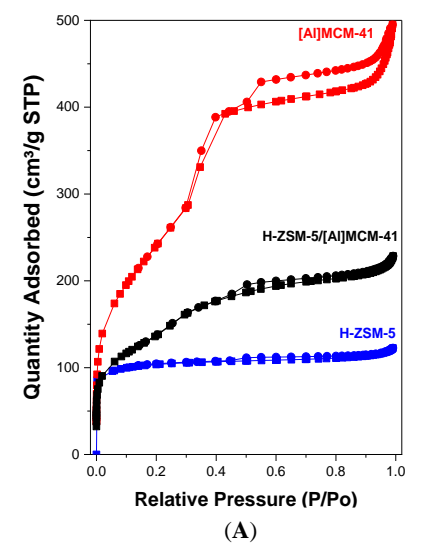
 ${\rm SiO_2/Al_2O_3}$ ratios were lower than the nominal value, suggesting that not all of the silica precursor was incorporated into the framework during synthesis. This discrepancy may be attributed to factors such as the reactivity and solubility of the silica source, synthesis conditions like gel composition and pH or kinetic limitations during crystallization.

In contrast, for [Al]MCM-41, the experimental SiO_2/Al_2O_3 ratio was slightly higher than expected, which could be due to incomplete incorporation of aluminum into the mesoporous framework, reported for others authors (12). This may result in the formation of extra-framework aluminum species or unreacted aluminum remaining in the synthesis medium. Additionally, deviations in both directions can also arise from analytical limitations, inhomogeneous distribution of aluminum within the material, or partial leaching during washing and calcination steps. Overall, such variations are frequently reported in the literature and do not necessarily compromise the structural integrity or functional performance of the synthesized materials (12-13).

Textural characterization

The textural properties of each synthesized material were determined by nitrogen adsorption—desorption isotherms and pore size distribution, as shown in Figure 4 and Table 2.

The H-ZSM-5 zeolite exhibits Type I isotherms, typical of microporous materials, with a large adsorption volume and small contributions from secondary mesopores due to the reaction of NaOH with the silica from the precursor material, promoting the interzeolite transformation of the H-Y zeolite (7). The [Al]MCM-41 and H-ZSM-5/[Al]MCM-41 samples show Type IV isotherms, associated with capillary condensation, typical of adsorption and desorption in mesoporous materials, with multilayer adsorption cycles (14).





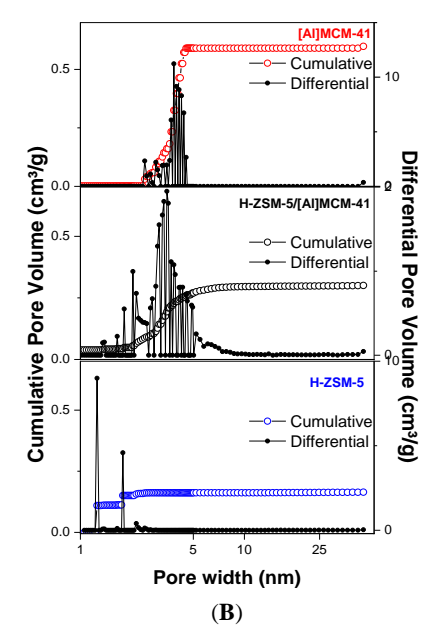


Figure 4. A: Nitrogen adsorption isotherms of materials; **B**: Pore distribution of the materials, by the NLDFT method.

For the [Al]MCM-41 material, a Type H4 hysteresis loop is observed, characteristic of [Al]MCM-41, suggesting cylindrical pores. However, the hybrid material does not show a prominent hysteresis loop, which may be related to the small particle size and the presence of pores around 4 nm. Additionally, small contributions from micropores are observed due to the incorporation of crystalline microporous zeolite during synthesis to produce hybrid materials, resulting in materials with a pore size distribution between microporous and mesoporous materials.

Figure 4.B shows the cumulative and differential pore volume for each sample. The [Al]MCM-41 displays a sharp and well-defined mesoporous distribution in the 2–5 nm range, which is characteristic of MCM-type materials. Among all samples, it exhibits the highest cumulative pore volume, highlighting its pronounced mesoporosity. H-ZSM-5 exhibits the lowest pore volume, predominantly microporous with minor mesoporous contributions, as expected for microporous zeolites. The hybrid material presents a bimodal pore distribution, with micropores (<2 nm) and mesopores (>2 nm), confirming its hybrid nature. Its pore volume is intermediate, resulting from the combination of the microporous H-ZSM-5 and mesoporous [Al]MCM-41 structures.



Table 2. Textural and porosity analysis of materials.

Samples	^a S _{BET} (m ² /g)	^b S _{NLDFT} (m ² /g)	bV _{micro} (cm ³ /g)	bV _{meso} (cm ³ /g)
H-ZSM-5	356	434	0,1150 (70,12%)	0,049 (29,88%)
[Al]MCM-41	854	1527	-	0,6027 (100%)
H-ZSM-5/ [Al]MCM-41	483	430	0,0485 (16,31%)	0,2488 (83,69%)

 $^{a}S_{BET}$: surface area calculated by the BET equation at P/P $_{0}$ = 0.05–0.2. $^{b}Pore$ size distribution, pore volume, and surface area determined by the NLDFT method.

Textural analysis by N_2 physisorption showed that the hybrid material exhibits a BET surface area of $483 \text{ m}^2 \text{ g}^{-1}$, intermediate between that of the H-ZSM-5 zeolite $(343 \text{ m}^2 \text{ g}^{-1})$ and the mesoporous [Al]MCM-41 material $(854 \text{ m}^2 \text{ g}^{-1})$. Pore size distribution by the NLDFT method revealed that 16.3% of the pore volume is attributed to micropores, while 83.7% corresponds to mesopores, as presented in Table 2.

Conclusions

Based on these results, it can be concluded that all materials were successfully synthesized. The crystallinity of the materials was confirmed by XRD analysis, also revealed the phases present after synthesis and demonstrated the structural stability of the materials after calcination, while their well-defined morphology was observed through SEM micrographs. The BET surface area of the hybrid material (483 m² g⁻¹) was intermediate between that of the microporous H-ZSM-5 zeolite (343 m²g⁻¹) and the mesoporous [Al]MCM-41 (854 m² g⁻¹). These results indicate that the hybrid structure successfully integrates the characteristics of both zeolitic and mesoporous materials, resulting in a material with balanced textural and structural properties. Furthermore, the combination of high surface area, structural integrity, and well-defined morphology suggests potential for catalytic applications.

Acknowledgements

J. Arce-Castro acknowledges CAPES for the scholarship granted. The authors also acknowledge the projects CATSUS-H₂ (CNPq, Process 405869/2022-3), USINA (FINEP, Process 0057/21), and FGTL (FINEP, Process 2435/22).



References

- Y. Liu; W. Zhang; T. J. Pinnavaia. J. Am. Chem. Soc. 2000, 122, 8791.
- 2. H. Kosslick; G. Lischke; G. Walther; W. Storek; A. Martin; R. Fricke. *Microporous Mater.* **1997**, *9*, 13–33.
- 3. T. Prasomsri; W. Jiao; S.Z. Weng; J. Garcia Martinez; *Chem. Commun.* **2015**, *51*, 8900–8911.
- 4. Y. Lui; T. J. Pinnavala. Chem. Matter. 2002, 14, 3.
- S. Ramírez; J. M. Domínguez; L. A. García; M. A. Mantilla; C. A. Flores; J. Salmones; D. Jerónimo. Petrol. Sci. Technol. 2004, 22, 119-127.
- 6. P.F. Corregidor, P.M. Cuesta, D.E. Acosta, H.A. Destéfanis, *Appl. Catal. A Gen.* **2019**, *587*, 117262.
- M.B. dos Santos, K.C. Vianna, H.O. Pastore, H.M. Andrade, A.J. Mascarenhas. *Micropor. Mesopor. Mat.* 2020, 306, 110413.
- 8. H.O. Pastore, M. Munsignatti, D.R. Bittencourt, M.M. Rippel. *Micropor. Mesopor. Mat.* **1999**, *32*, 211.
- 9. J.C. Vartuli; W.J. Roth; J.S. Beck; S.B. McCullen; C.T. Kresge. *in Synthesis*, Springer Berlin Heidelberg, **2001**, 97.
- N. La-Salvia; J.J. Lovón-Quintana; A.S.P. Lovón; G.P. Valenca. *Mater. Res.* 2017, 20, 1461.
- 11. J.M.D. Cónsul; C.A. Peralta; E.V. Benvenutti; J.A. Ruiz; H.O. Pastore; I.M. Baibich. *J. Mol. Catal. A: Chem.* **2006**, *246*, 33.
- 12. S. C. Shen, S. Kawi, Langmuir. 2002, 18, 4720.
- R. E. Yakovenko, I. N. Zubkov, V. G. Bakun, A. N. Shmakov, A. I. Boronin, V. V. Lunin. *Pet. Chem.* 2022, *62*, 101.
- 14. J. Rouquerol; F. Rodríguez-Reinoso; K.S.W. Sing. *Characterization of Porous Solids III*, Elsevier, Amsterdam, **1994**.